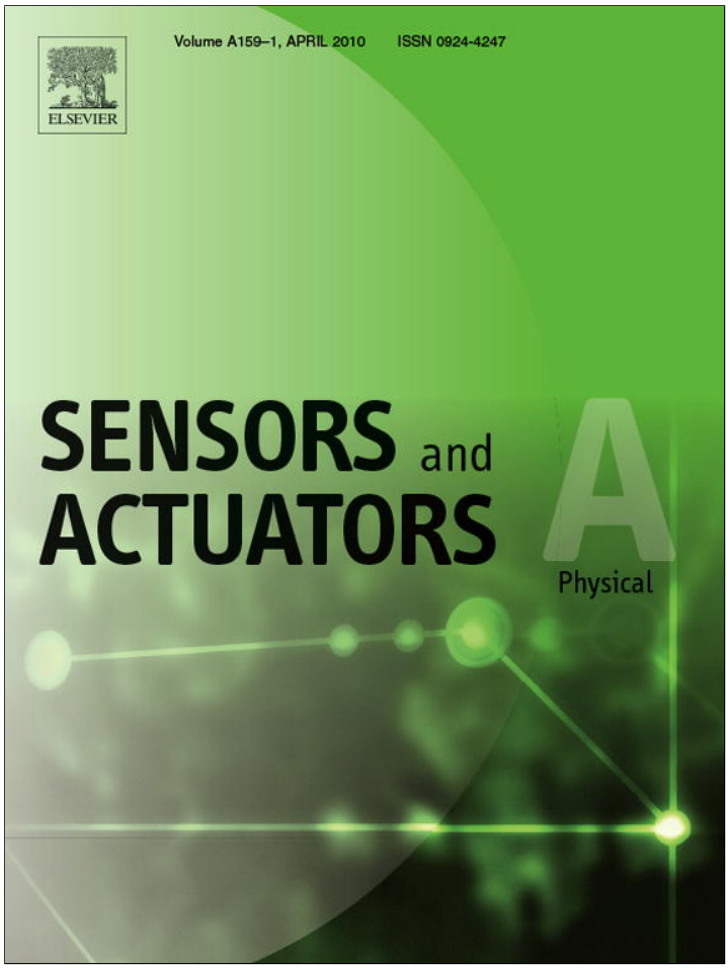

Sensors and Actuators A 159 (2010) 88–95

Contents lists available at ScienceDirect

Sensors and Actuators A: Physical

journal homepage: www.elsevier.com/locate/sna

Effects of residual stresses on lead–zirconate–titanate (PZT) thin-film membrane microactuators

Cheng-Chun Lee[a], G.Z. Cao[b], I.Y. Shen[a,*]

[a] Department of Mechanical Engineering, University of Washington, Seattle, WA 98195-2600, USA
[b] Department of Material Science & Engineering, University of Washington, Seattle, WA 98195-2120, USA

ARTICLE INFO

Article history:
Received 25 September 2009
Received in revised form 17 February 2010
Accepted 18 February 2010
Available online 1 March 2010

Keywords:
PZT thin films
Membrane microactuators
Actuator displacement
Residual stresses
Finite element analysis
DC bias voltage

ABSTRACT

A common design of piezoelectric microactuators adopts a membrane structure that consists of a base silicon structure, a layer of bottom electrode, a layer of piezoelectric thin film, and a layer of top electrode. In particular, the piezoelectric thin film is often made of lead–zirconate–titanate (PZT) for its high piezoelectric constants. When driven electrically, the PZT thin film extends or contracts flexing the membrane generating an out-of-plane displacement. For PZT thin-film microactuators, residual stresses are unavoidable from fabrication and can significantly reduce the actuation displacement. In this paper, the authors present a fourfold approach to address the issue of residual stresses. First, we demonstrate experimentally that two PZT thin-film actuators may present substantially different displacement and natural frequency even though dimensions of the two actuators are similar. Through a series of finite element analyses, we conclude that only residual stresses can produce such a significant frequency shift reducing the displacement of a PZT thin-film microactuator. Second, we measure the warping of the PZT thin-film actuator via interferometry to detect residual stresses. A simple calculation using shell theories indicates that the warping only causes a tiny shift in natural frequencies. Therefore, most of the degradation of actuator performance results from the nature that residual stresses are in-plane rather than the warping caused by the residual stresses. Third, we develop a vibration analysis to determine when residual stresses could significantly reduce actuator displacement. Fourth, we demonstrate two simple ways to mitigate the negative effects of residual stresses: poling at an elevated temperature and applying a DC bias voltage.

1. Introduction

PZT thin-film microactuators have a wide range of applications, such as scanning mirrors [1], hard disk drive read/write heads [2], micro pumps and valves [3], and radio-frequency switches [4]. These microactuators usually take the form of cantilevers, bridges, and membranes.

For a PZT thin-film membrane microactuator, it typically consists of four parts: a membrane, a bulk silicon substrate, a PZT thin-film layer, and a pair of electrodes, see Fig. 1. (Note that the parts in Fig. 1 are not drawn in proportion.) The membrane is a moving component of the actuator anchored to the silicon substrate. As a result of its small thickness, the silicon membrane has low structural stiffness compared with the substrate. Often, the membrane can be fabricated by releasing part of the bulk silicon substrate. On top of the membrane is a layer of PZT thin film with a pair of electrodes. When a driving voltage is applied to the electrodes, the PZT thin film extends or contracts in the plane of the membrane, thus creating a bending moment to flex the membrane out of its plane. Such PZT thin-film membrane actuators have appeared in many applications including micro pumps [5], deformable mirrors [6], micro speakers [7], energy harvesters [8], and hybrid cochlear implant actuators [9].

In fabricating these PZT thin-film devices, presence of residual stresses is unavoidable if the films are fabricated via sol–gel processes [10–13]. Stresses arise when the PZT thin film loses its solvent and shrinks substantially during the sintering process (for example, 650 °C). Stresses also occur when the PZT film goes through a phase transformation from the pyrochlore to the perovskite structure to exhibit piezoelectric properties. Moreover, the PZT thin film has a distinct coefficient of thermal expansion (CTE) from that of the substrate layers. As a result, a large temperature drop from the sintering temperature to the room temperature induces significant thermal residual stresses in the PZT thin films. The lattice mismatch between the PZT thin film and the substrate, as well as the domain rotation of PZT, further contributes to the residual stresses. In general, the residual stresses are difficult to predict, estimate, and control.

* Corresponding author. Tel.: +1 206 543 5718; fax: +1 206 685 8047.
E-mail address: ishen@u.washington.edu (I.Y. Shen).

0924-4247/$ – see front matter © 2010 Elsevier B.V. All rights reserved.
doi:10.1016/j.sna.2010.02.022

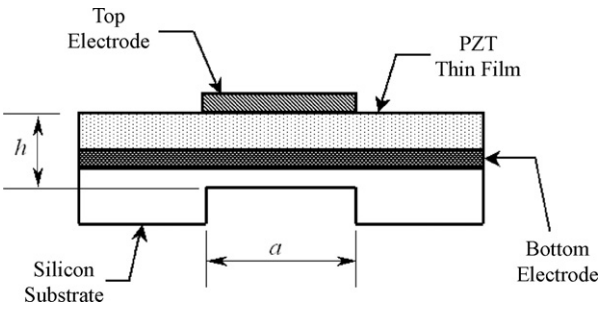

Fig. 1. Schematic drawing of PZT thin-film membrane actuator (not in proportion).

In the last decade, many researchers have found that residual stresses can significantly affect electromechanical properties [10] or piezoelectric properties [14,15] of PZT thin films. These research efforts primarily focus on material properties from a viewpoint of material science. In a PZT thin-film microdevice, many researchers have found that the presence of residual stresses can warp the surface of the microdevice [16–18]. For sensor applications, the warping can degrade sensor sensitivity significantly [16,17]. For actuator applications, it remains open whether or not residual stresses and the subsequent warping would adversely affect performance of PZT thin-film microactuators. If so, in what way do residual stresses degrade actuator performance? Under what condition will residual stresses adversely affect actuator performance? What are available avenues to mitigate residual stresses to improve actuator performance?

The purpose of this paper is to answer these questions and demonstrate that residual stresses could indeed adversely affect performance of a PZT thin-film membrane microactuator in terms of actuator natural frequency and displacement. The paper consists of four parts that are closely interrelated. In the first part, we demonstrate experimentally that two PZT thin-film actuators may present substantially different displacement and natural frequency even though dimensions of the two actuators are similar. Through a series of finite element analyses, we conclude that only residual stresses can produce such a significant frequency shift reducing the displacement of a PZT thin-film microactuator. In the second part, we measure the warping of the PZT thin-film actuator via interferometry. A simple calculation using shell theories indicates that the warping only causes a limited shift in natural frequencies. Therefore, most of the degradation of actuator performance results from the nature that residual stresses are in-plane rather than the warping caused by the residual stresses. In the third part, we develop a vibration analysis to determine when residual stresses could significantly reduce actuator displacement. In the last part, we demonstrate two simple ways to mitigate the negative effects of residual stresses: poling at an elevated temperature and applying a DC bias voltage.

2. Measurements of actuator performance

Recently, some experimental results from the authors' research suggest that residual stresses could adversely reduce the displacement of a PZT thin-film actuator. Fig. 2 shows measured results from two comparable PZT thin-film membrane microactuators following the same fabrication process described in [19]. The diaphragm size is 800 μm by 800 μm, and the thickness of the diaphragm is about 2 μm (about 1 μm for PZT and 1 μm for silicon). Fig. 2(a) compares the etching from the backside. Note that both microactuators are etched to almost the same condition with roughly the same diameter of remaining silicon.

The PZT thin film is poled at about 20 V for 30 min. After poling, the actuators are driven by 5 V at 3 kHz via a function generator and an AVC amplifier. The displacement at the center point of the actuator is measured via a laser Doppler vibrometer (LDV). Fig. 2(b) compares the measured displacement of the two microactuators. As shown in Fig. 2(b), one microactuator shows a sensitivity of around 30 nm/V, while the other shows only about 5 nm/V. There are two possible sources that could cause the large disparity of actuator sensitivity. First, the two actuators have very different piezoelectric constants. Second, the two actuators have very different stiffness.

To identify the source of the drastic difference, we further measure natural frequencies of the two microactuators. The experimental setup consists of a spectrum analyzer, an AVC amplifier, and an LDV. The spectrum analyzer generates a random signal driving the PZT actuator through use of the AVC amplifier. In the meantime, the LDV measures velocity of the center point of the actuator. Both driving voltage and LDV measurement are fed into the spectrum analyzer to calculate frequency response functions, whose resonance frequencies identify the natural frequencies of the PZT thin-film actuator.

Fig. 2(c) compares the measured frequency response functions of the two microactuators. Experimental results indicate that the microactuator with small displacement (5 nm/V) has much larger natural frequency (equal to or larger than 100 kHz). The experimental results lead to the following two conclusions. First, difference in piezoelectric constants is not the major cause of the disparity between the actuator sensitivity, because piezoelectric constants determine forced response and do not affect natural frequencies significantly. Second, the small actuator displacement results from the large natural frequency. This implies that the disparity in actuator sensitivity results from the actuator stiffness.

3. Finite element analyses

In this section, we adopt a finite element model developed by Lee et al. [20] for a PZT thin-film membrane actuator to identify where the significant frequency difference comes from. The finite element model consists of a gold layer, a PZT layer, and a single Pt/silicon layer to represent the multi-layered actuator structure. The finite element model also includes the remaining silicon in Fig. 2(a), which was a result of non-uniform etching. Furthermore, a linear analysis is performed to predict natural frequencies of the membrane structure.

We take a two-pronged approach in the finite element analysis. First, we measure exact dimensions as well as natural frequencies of several microactuators. We also measure the piezoelectric constant d_{33} and Young's modulus of the PZT thin film. The exact dimensions and material properties are then used as FEA input, while the natural frequencies can be used for FEA comparison. Second, we conduct a parametric study by varying actuator dimensions and residual stresses to determine which parameter could significantly affect the natural frequencies. The detail of our study is explained as follows.

3.1. Measurements of dimensions and material properties

The thickness of each layer of the PZT thin-film actuator is measured via an SEM. The PZT actuators are first diced from a whole wafer, and the individual actuators are engraved with a diamond scriber over the bulk silicon portion and cleaved into halves. The samples are further evaporate-coated with a gold and palladium alloy of 30 nm for better observation. Distinct Au, PZT, Ti/Pt and $Si/SiO_2/SiN_x$ layers are observed in the SEM pictures; see Fig. 3.

Table 1 lists major dimensions of three actuators of interest fabricated from the same wafer. The dimensions are measured so that the SEM is perpendicular to the Au layer while measuring the

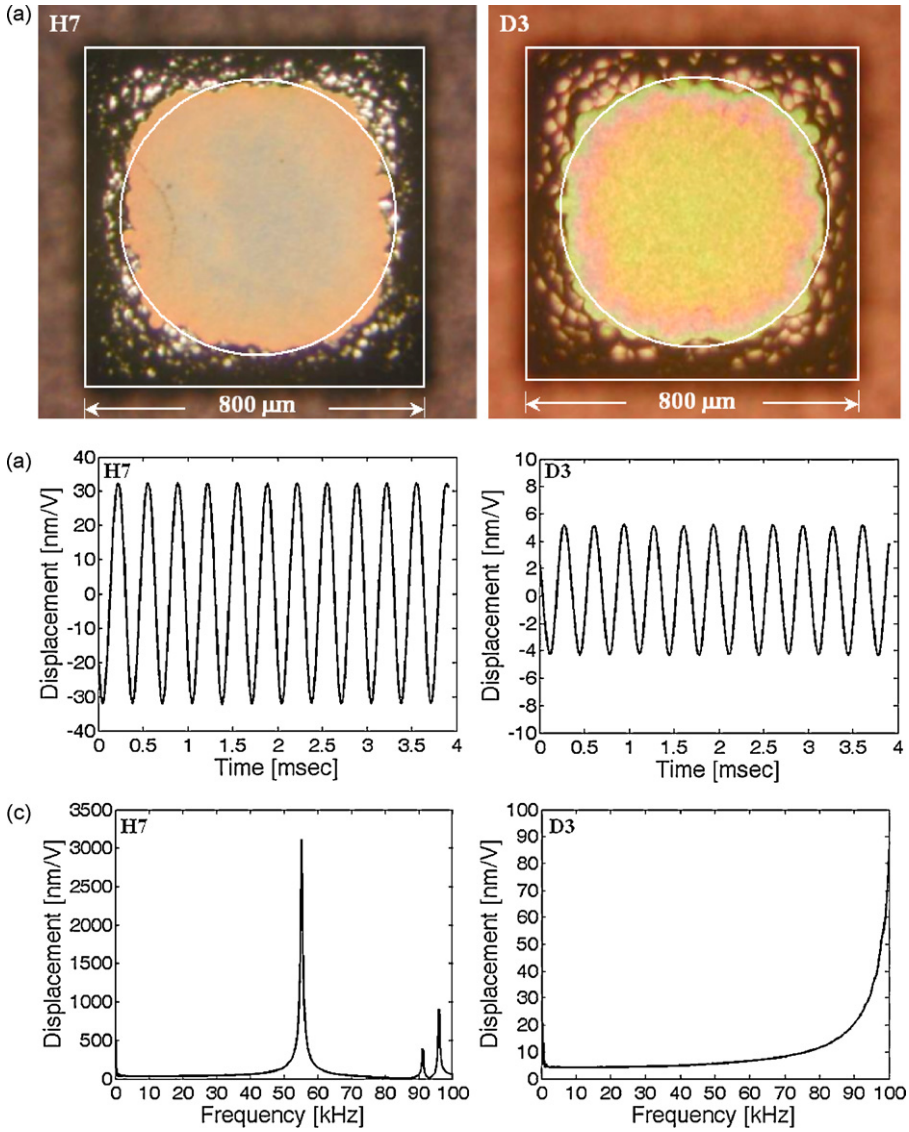

Fig. 2. (a) backside etching, (b) sensitivity, and (c) frequency response of two microactuators.

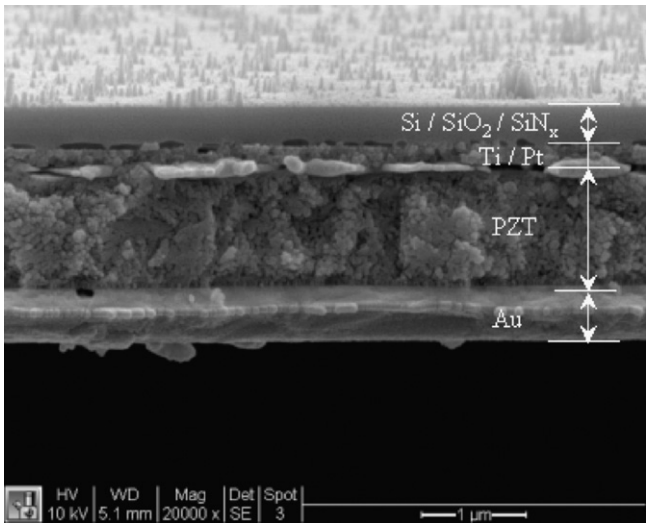

Fig. 3. Layered structure observed under SEM.

Table 1
Measured dimensions of three PZT actuators (from the same wafer).

Actuator number	$Si/SiO_2/SiN_x$ (μm)	Ti/Pt (μm)	PZT (μm)	Au (μm)
B3	0.45	0.21	1.15	0.58
C4	0.48	0.19	1.00	0.53
A7	0.54	0.22	0.94	0.52

Au thickness, and is perpendicular to the $Si/SiO_2/SiN_x$ layers while measuring these layers. If the SEM is oriented such that it is perpendicular to the $Si/SiO_2/SiN_x$ layers while measuring the Au thickness, or vice versa, the measured dimensions can vary by 10–20%.

In addition, the Young's modulus of the PZT film is 70 GPa measured via nano-indentation. The piezoelectric constant d_{33} is 9 pC/N measured via a mini-hammer, a load cell and an oscilloscope [21].[1]

[1] Note that the measured d_{33} is somewhat low, but its value will not have a significant effect on the predictions of natural frequencies.

Table 2
Comparison of natural frequencies.

Actuator number	Experiment (Hz)	FEA (Hz)	Ratio (FEA/Exp)
B3	92,878	47,899	0.52
C4	59,578	39,574	0.66
A7	96,059	50,577	0.53

3.2. Predicted vs. measured natural frequencies

The measured dimensions in Table 1 along with the measured material constants are used as input to the FEA model to predict natural frequencies. Table 2 (the third column) lists the predicted natural frequencies, which are in the range of 40–50 kHz. In contrast, the second column in Table 2 lists the measured natural frequencies for comparison (using the same experimental setup leading to Fig. 2(c)). The measured frequencies are in the range of 60–100 kHz.

We can see that the natural frequencies calculated from the FEA are consistently smaller than those from the LDV measurement, often in the order of 50–65%. The wide discrepancy indicates that the current finite element model lacks one or more critical factors in modeling the PZT thin-film membrane actuators.

To seek the critical parameter, we identify a list of possible factors and conduct a parametric study. Via a series of finite element analysis, we can evaluate how much each factor affects natural frequencies. Note that material properties of the PZT film are not likely critical factors, because Young's modulus and piezoelectric constant of the film have been measured. Furthermore, density of the PZT thin film is not likely a critical factor either, because the inertia force is small and does not affect the displacement of the microactuator. In the end, two possible factors are identified: uncertainties in actuator dimensions and residual stresses.

3.3. Effects of dimension uncertainties

As explained earlier, there are uncertainties in the SEM measurements of the thickness of each layer of the PZT actuator. To understand the influence of these measurement uncertainties, we conducted an FEA parametric study by varying the thickness of the Si and the Au layers, while keeping the thickness of the PZT layer constant. Specifically, we use actuator C4 as an example for demonstration as follows.

In this parametric study, the PZT film is assumed to have a thickness of 1 μm (cf. Table 1). The silicon layer and the bottom electrode are combined into a single layer with a composite Young's modulus of 150 GPa. In addition, its thickness is varied from 0.2 μm to 2.5 μm. A modal analysis is conducted to predict the lowest natural frequency. In Fig. 4, the solid line represents the predicted natural

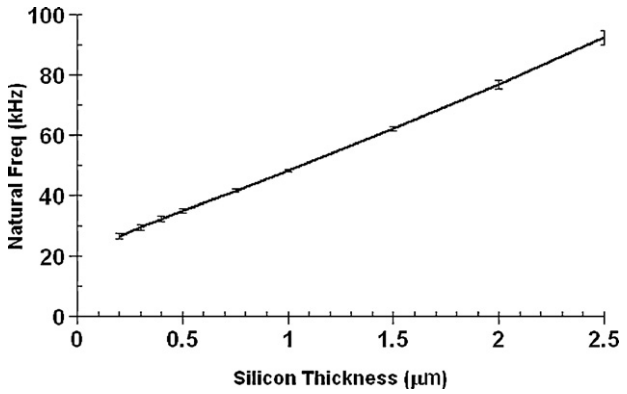

Fig. 4. Natural frequencies vs. layer thickness for actuator C4.

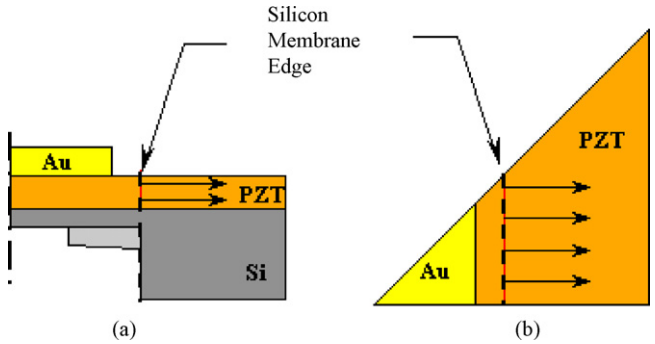

Fig. 5. Application of an external pre-stress to simulate residual stresses on the PZT membrane actuator; (a) side view and (b) top view.

frequency, when the Au layer has a thickness of 0.5 μm. In addition, the error bars represent the change of the natural frequency, if the thickness of the Au layer is varied from 0.3 μm to 0.7 μm. As one can tell from Fig. 4, the thickness of the Au layer has very little effect on the natural frequency, because the error bars are extremely narrow.

According to Table 1, the combined thickness of the silicon and the bottom electrode is roughly 0.7 μm for actuator C4, in which 0.5 μm results from the silicon layer and 0.2 μm results from the Pt bottom electrode. The measurement of the silicon layer thickness may vary 20% as mentioned earlier. As a result, the thickness of the combined layer should be within 0.55 μm and 0.85 μm for actuator C4. Correspondingly, the predicted natural frequency in Fig. 4 varies from 36 kHz to 45 kHz, whereas the measured natural frequency of actuator C4 is about 60 kHz. This shows that the dimension uncertainty is not a critical factor in the finite element analysis. The same result is observed for the other two actuators B3 and A7.

3.4. Effects of residual stresses

Another parameter that can significantly alter the nature frequencies is residual membrane stresses. Residual stresses arise in MEMS processes when two materials with different coefficients of thermal expansion (CTE) are layered to each other [22,23]. The effect is especially significant if such processes take place at a high temperature, such as sintering in the PZT sol–gel process. Since the PZT thin-film actuator incorporates a multi-layer structure, residual stresses in the actuator are extremely complex. As a first approximation, we simulate the residual stresses in our FEA model by applying a uniform in-plane pre-stress in the PZT layer along the edge of the silicon substrate; see Fig. 5. Since the finite element model is a one-eighth model of the actuator, the uniform pre-stress in Fig. 5 corresponds to a biaxial stress state with $\sigma_x = \sigma_y = p$, where σ_x and σ_y are the stresses in the plane of the membrane and p is the constant pre-stress applied. Since the biaxial stress state is hydrostatic (i.e., $\sigma_x = \sigma_y$), only 1 stress component is needed to describe the stress state in this finite element model.

Again, let us use actuator C4 to demonstrate the effect of residual stresses. In the simulation, let the applied pre-stress p vary from 0 MPa to 500 MPa. Due to the presence of the silicon substrate and remaining silicon, the corresponding hydrostatic membrane stress σ developed inside the PZT layer at the center of the membrane actuator ranges from 0 MPa to 7 MPa. Fig. 6 shows how the membrane stress σ affects the natural frequency of actuator C4. Since the membrane stress is tensile, it has a stiffening effect. When the membrane stress σ reaches 6.2 MPa, the natural frequency of the actuator increases to 59.07 kHz for actuator C4, which is very close to the measured frequency shown in Table 2.

We have also repeated the simulations for the other two actuators B3 and A7. Table 3 lists the results for comparison. For B3, a

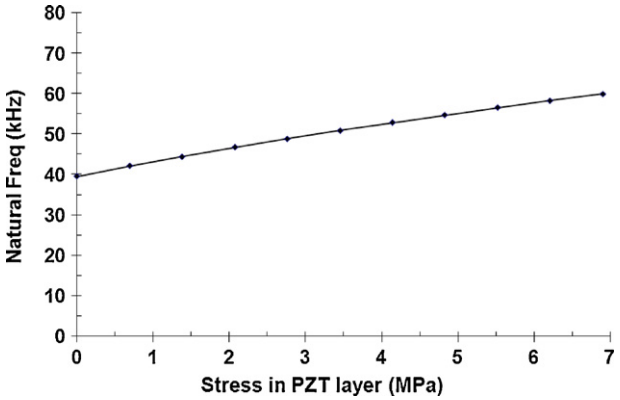

Fig. 6. Natural frequencies as a function of the pre-stress for actuator C4.

Table 3
Comparison of natural frequencies predicted from the pre-stress model.

Actuator number	Experiment (Hz)	FEA from pre-stress model (Hz)	Membrane stress σ (MPa)
B3	92,878	92,890	17.6
C4	59,578	59,070	6.2
A7	96,059	96,640	18.6

membrane stress of 17.6 MPa will increase the natural frequency to 92.89 kHz. For A7, a membrane stress of 18.6 MPa will increase the natural frequency to 96.64 kHz. The finite element simulation thus indicates that the membrane stress σ is a critical parameter that can correct the discrepancy between the theoretical predictions and the experimental measurements in natural frequency.

There are several issues worth noting for this finite element simulation of residual stresses. First, the model in Fig. 5 is an extremely simple model leading to a hydrostatic stress state that is characterized by a single membrane stress σ. In reality, the residual stresses will be much more complicated and require substantial further study. Second, the significant frequency difference shown in Table 2 can only be matched when the membrane stress is tensile. In this model, compressive residual stresses would reduce the natural frequencies and thus increase the actuator displacement, which was not observed in the experiments.

4. Surface warping

Since the membrane actuator has small thickness and thus small bending rigidity, the presence of residual stresses could lead to significant warping of the membrane surface. This often occurs when the membrane is released from a bulk structure during the fabrication [24–26]. Therefore, experimentally measured surface warping can serve as an indirect evidence of significant residual stresses.

To measure the surface warping, we scan the membrane surface using a Wyco optical profiler (model NT3300). As shown in Fig. 7, the surface takes the shape of a dome. The top of the dome is 0.376 μm above the general plane surface. Since the thickness of the membrane is about 2 μm, the warping is almost 20% of the thickness. This indicates a significant surface warping as a result of a significant residual stress field.

In thin shell theories, warping of a surface could increases the stiffness resulting in increased natural frequency. According to [27], natural frequencies of a curved shell and a flat plate are related via

$$\omega_{\text{curve}}^2 = \omega_{\text{flat}}^2 + \frac{E}{\rho R^2} \tag{1}$$

where ω_{curve} is the natural frequency of a curved shell, ω_{flat} is the natural frequency of the original flat shell, E is the Young's modulus, ρ is the density, and R is the radius of curvature of the shell, respectively.

We can use Eq. (1) to check whether or not the warping of the actuator surface causes the significant discrepancy in measured and predicted natural frequency as follows. First, we need to estimate

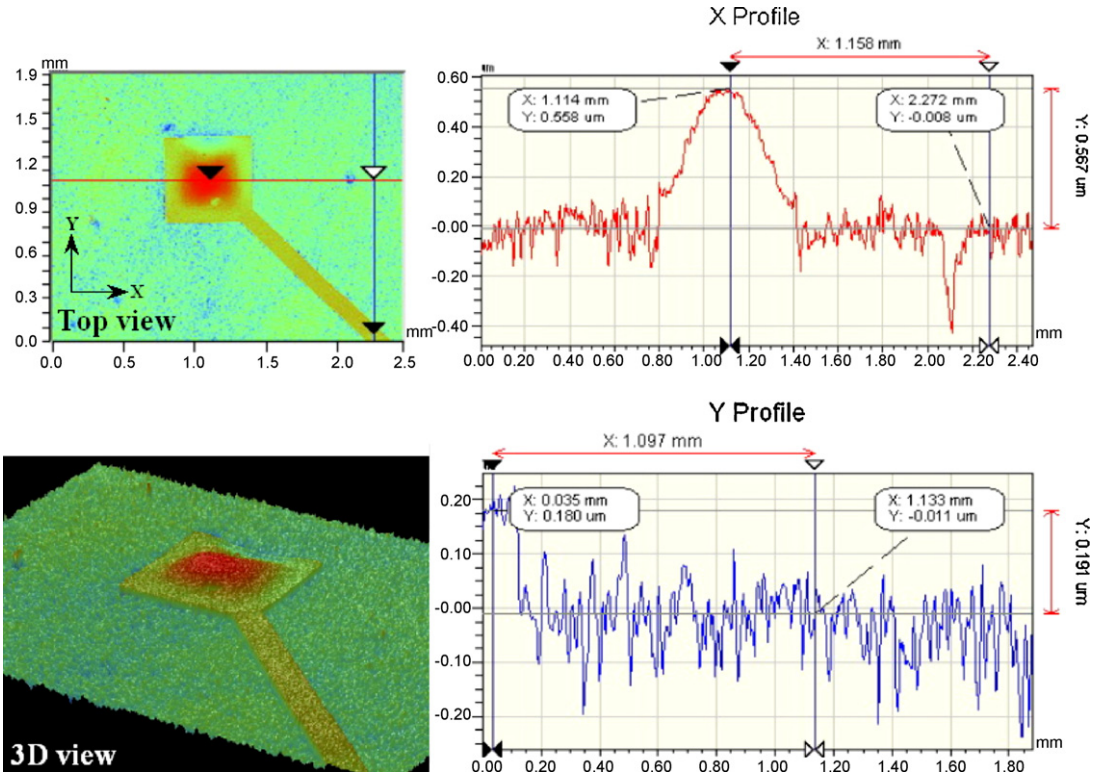

Fig. 7. Profile of a PZT membrane actuator.

the radius of curvature of the warped surface. Let R, s, and d be the radius of curvature, height and diameter of the domed surface, respectively. Basic geometry leads to

$$R^2 = (R-s)^2 + \left(\frac{d}{2}\right)^2 \tag{2}$$

or

$$R = \frac{s}{2} + \frac{1}{2s}\left(\frac{d}{2}\right)^2 \tag{3}$$

From our measurements, s is 0.376 μm and d is the diameter of the residual silicon from the backside of the actuator, which is 590 μm. The radius of curvature R of the warped surface calculated from Eq. (3) is 0.116 m.

The next step is to use Eq. (1) to calculate the frequency shift as a result of the warped surface. As a back-of-the-envelope calculation, we can assume that E is 100 GPa, ρ is 2700 kg/m^3, and ω_{flat} is 50 kHz. With Eq. (1) and R being 0.116 m, the natural frequency of the warped surface is roughly 50.7 kHz. In other words, the estimated natural frequency shift will be less than 1 kHz. Therefore, the warping of the surface does not cause the significant difference between the predicted and measured natural frequencies. The difference results from the in-plane membrane stresses.

5. Vibration analysis

With the evidence from the finite element analyses and Wyco measurements, it is important to assess when residual stresses could significantly affect natural frequencies reducing the actuator displacement. This can be done through a simple vibration analysis as follows.

In this analysis, the PZT thin-film actuator is modeled as a square elastic plate with in-plane membrane stresses for simplicity. The square plate is located on the xy plane, while the z axis defines the out-of-plane direction. Let the length and thickness of the square plate be a and h, respectively; see Fig. 1. Also, the square plate has Young's modulus E, Poisson ratio ν and mass per unit area ρ. In addition, the square plate is subjected to internal in-plane hydrostatic normal stress σ. Out-of-plane displacement $w(x, y, t)$ of the plate then satisfies,

$$-\frac{Eh^3}{12\left(1-\nu^2\right)}\nabla^4 w + \sigma h \nabla^2 w + p(x,y,t) = \rho\frac{\partial^2 w}{\partial t^2} \tag{4}$$

where $\nabla^2 \equiv (\partial^2/\partial x^2) + (\partial^2/\partial y^2)$ is the harmonic operator, and $p(x,y,t)$ is external loading on the plate (e.g., bending moments from the PZT actuation). Also note that $-(Eh^3/12(1-\nu^2))\nabla^4 w$ in (4) results from bending rigidity of the plate, while $\sigma h\ ^2 w$ results from the in-plane residual stresses. Moreover, xy axes are along two neighboring orthogonal edges of the square membrane with the origin being a corner of the membrane.

Let ω be a natural frequency of the membrane actuator and $W(x,y)$ be the corresponding mode shape. The natural frequency can be estimated via the Rayleigh quotient from Eq. (4), i.e.,

$$\omega^2 = \frac{\frac{Eh^3}{12(1-\nu^2)}\int W\nabla^4 W dA - \sigma h\int W\nabla^2 W dA}{\rho\int W^2 dA} \tag{5}$$

where the integration is carried out over the entire domain of the square plate (i.e., $dA \equiv dxdy$). According to (5), the residual stresses will not significantly affect the natural frequencies if

$$-\sigma h\int W\nabla^2 W dA \ll \frac{Eh^3}{12(1-\nu^2)}\int W\nabla^4 W dA \tag{6}$$

For the first mode that we measure in Fig. 2, the mode shape $W(x,y)$ can be approximated as

$$W(x,y) = \sin\frac{\pi x}{a}\sin\frac{\pi y}{a} \tag{7}$$

Substitution of (7) into (6) then leads to

$$\sigma \ll \frac{E\pi^2}{6(1-\nu^2)}\left(\frac{h}{a}\right)^2 \tag{8}$$

For the PZT thin-film membrane actuator discussed in this paper, $h \approx 2$ μm and $a \approx 800$ μm. The membrane actuator is half silicon ($E \approx 150$ GPa) and half PZT ($E = 70$ GPa); therefore, the average Young's modulus can be approximated as $E = 110$ GPa. If Poisson ratio ν is assumed to be 0.3, Eq. (8) estimates that the residual stresses must be

$$\sigma \ll \frac{110\times 10^9 (3.1416)^2}{6\left(1-0.3^2\right)}\left(\frac{2}{800}\right)^2 \approx 1.243\ \text{MPa} \tag{9}$$

in order not to significantly affect the natural frequency.

There are various ways to verify the predictions in (8) and (9). For example, Yao et al. [28] calculated residual stresses of sol–gel derived PZT films from XRD measurements. The stress in the PZT film can range from 36 MPa to 320 MPa depending on the assumptions used. Both stress calculations indicate that the residual stress has exceeded the allowable stress in (9) and a significant shift in natural frequency is likely.

Alternatively, one can do a back-of-the-envelop calculation to estimate the magnitude of residual stresses in the membrane as follows. The PZT thin film (with 1-μm thickness) is sintered on a silicon wafer (with 400-μm thickness) at 650 °C, and subsequently cooled down to room temperature. Let us assume that the PZT-Si system behaves like a bimetallic plate. According to basic mechanics of material, the thermal stresses in the PZT film will be

$$\sigma_{\text{PZT}} = \frac{E_{\text{PZT}}\Delta\alpha\Delta T}{1+(E_{\text{PZT}}h_{\text{PZT}}/E_{\text{Si}}h_{\text{Si}})} \tag{10}$$

and the thermal stresses in the silicon will be

$$\sigma_{\text{Si}} = \frac{E_{\text{Si}}\Delta\alpha\Delta T}{1+(E_{\text{Si}}h_{\text{Si}}/E_{\text{PZT}}h_{\text{PZT}})} \tag{11}$$

where $\Delta\alpha$ is the mismatch of coefficients of thermal expansion between PZT and Silicon, and ΔT is the temperature change. If $\Delta\alpha$ is assumed to be 1×10^{-6}/°C (tiny thermal mismatch) and $\Delta T \approx 600$ °C, the stresses in the PZT film from (10) will be roughly 42 MPa. This thermal stress is significantly larger than the allowable 1.243 MPa from Eq. (9). This simple back-of-the-envelop calculation also indicates that thermal stresses can easily cause natural frequency to increase thus limiting the displacement of the PZT thin-film microactuator.

6. Mitigation of residual stresses

According to the experimental evidence, finite element analyses and vibration analyses above, residual stresses can affect the natural frequency and displacement of the PZT thin-film membrane actuator significantly. In this section, we introduce two simple ways to mitigate the negative effect of residual stresses. They are poling at elevated temperatures and DC bias voltage. The basic idea is to alter the stress state thus obtaining a better actuator performance.

During the poling process, we divide the specimens into four batches. The first batch is poled with 21 V at room temperature for 30 min (denoted as no-HP). The second batch is poled with 21 V on a hot plate at 100 °C for 30 min (denoted as HP-30). The third batch is poled with 21 V on a hot plate at 100 °C for 60 min (denoted as HP-60). The fourth batch is poled with 21 V on a hot plate at 100 °C for 90 min (denoted as HP-90).

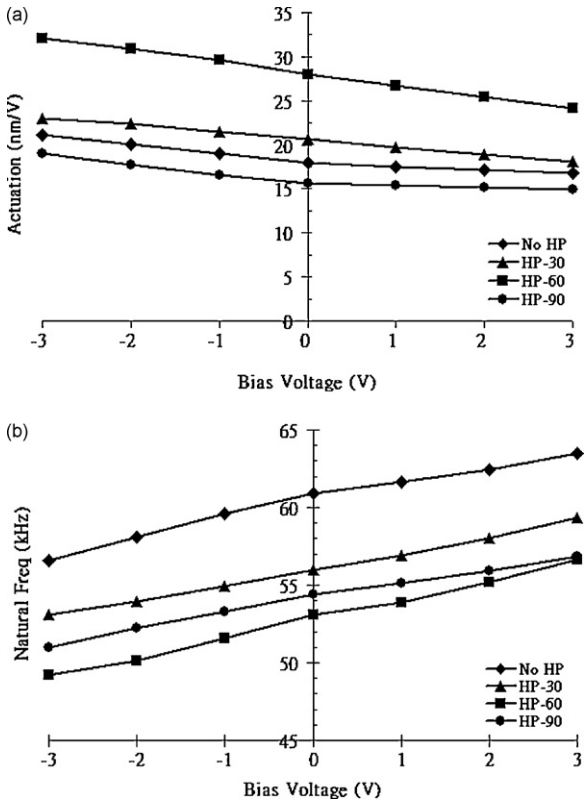

Fig. 8. (a) Actuator sensitivity (displacement per volt) with respect to DC bias voltage and (b) first natural frequencies with respect to DC bias voltage.

After the poling, we drive the PZT thin-film membrane actuator with a voltage of:

$$V(t) = V_0 + V_1 \sin 2\pi\omega t \quad (12)$$

where V_0 is a DC bias voltage in the same direction as the poling voltage and ω is a driving frequency (3 kHz in our experiments). Moreover, the driving and bias voltages combined were controlled such that the maximum voltage did not exceed one-third of the poling voltage.

Fig. 8(a) and (b) illustrates how measured actuator displacement (per unit volt of V_1) and actuator frequency vary with respect to the bias voltage V_0 for all three poling conditions. There are several important phenomena worth noting.

First, poling at the elevated temperature could significantly increase the actuator displacement. When the specimen is poled at 100 °C for 60 min, the actuator displacement without a bias voltage increases from 18 nm/V to 28 nm/V, which is about 50% increase. The elevated temperature might have altered the residual stresses and realign domain directions in the PZT film during the poling process. Nevertheless, poling at an elevated temperature for an extended period does not necessary help. For example, if the poling is held at 100 °C for 90 min, the actuator displacement is dropped to 16 nm/V. The experiments have been repeated several times, and this phenomenon has been observed for many samples. There is an unknown mechanism behind this phenomenon, and it requires further studies.

Second, the presence of the bias voltage can improve the actuator displacement. For example, when the sample is poled at room temperature, a 3 V DC bias can improve the actuator displacement from 18 nm/V to about 21 nm/V (a margin of 15%). The same improvement is also observed for specimens poled at elevated temperature. The bias voltage, however, can decrease the actuator displacement, if the polarity of the voltage is wrongly applied.

Third, comparison of Fig. 8(a) and (b) shows that the bias voltage and the poling process can significantly alter the natural frequency and thus the actuator displacement. In general, the increase of the natural frequency corresponds to the decrease of actuator displacement (except the case of HP-90).

7. Conclusions

In this paper, we demonstrate that residual stresses can significantly increase the natural frequency and reduce the displacement of a PZT thin-film membrane actuator. We demonstrate this fact through experimental measurements, finite element analyses together with a vibration analysis and several back-of-the-envelop calculations. As a result, Eq. (8) can serve as a first approximation to check whether or not the residual stresses are large enough to affect actuator displacement. In additional, warping of the actuator surface does not seem to be a main contributor in reducing actuator displacement. Finally, poling at elevated temperature and application of a DC bias voltage are two simple ways to mitigate the negative effects of residual stresses.

Acknowledgments

This material is based upon work supported by the National Science Foundation under Grant No. CMMI-0826501. Any opinions, findings, and conclusions or recommendations expressed in this material are those of the authors and do not necessarily reflect the views of the National Science Foundation.

References

[1] W. Lin, A. Schroth, S. Matsumoto, C. Lee, R. Maeda, Two-dimensional microscanner actuated by PZT thin film, Proceedings of the SPIE 3892 (1999) 133–140.
[2] K. Suzuki, R. Maeda, J. Chu, T. Kato, M. Kurita, An active head slider using a piezoelectric cantilever for in situ flying-height control, IEEE Transactions on magnetics 39 (2) (2003) 826–831.
[3] R. Maeda, J. Tsaur, S. Lee, M. Ichiki, Piezoelectric microactuator devices, Journal of Electroceramics 12 (2004) 89–100.
[4] S. Gross, S. Tadigadapa, T. Jackson, S. Trolier-McKinstry, Q. Zhang, Lead–zirconate–titanate-based piezoelectric micromachined switch, Applied Physics Letters 83 (1) (2003) 174–176.
[5] K. Brooks, D. Damjanovic, A. Kholkin, I. Reaney, N. Setter, P. Luginbuhl, G. Racine, N. Rooij, A. Saaman, PZT films for micro-pumps, Integrated Ferroelectrics 8 (1) (1995) 13–23.
[6] Y. Hishinuma, E. Yang, Piezoelectric unimorph microactuator arrays for single-crystal silicon continuous-membrane deformable mirror, Journal of Microelectromechanical systems 15 (2) (2006) 370–379.
[7] S. Ko, Y. Kim, S. Lee, S. Choi, S. Kim, Piezoelectric membrane acoustic devices, in: The 15th IEEE international conference on Micro Electro Mechanical Systems, 2002, pp. 296–299.
[8] J. Cho, M. Anderson, R. Richards, D. Bahr, C. Richards, Optimization of electromechanical coupling for a thin-film PZT membrane. II. Experiment, Journal of Micromechanics and Microengineering 15 (2005) 1804–1809.
[9] C. Lee, C. Hume, G. Cao, I. Shen, A feasibility study of PZT thin-film microactuators for hybrid cochlear implants, in: Proceedings of the 2005 27th Annual International Conference of the Engineering in Medicine and Biology Society, IEEE-EMBS, 2005, pp. 1929–1932.
[10] L. Lian, N.R. Sottos, Stress effects in sol–gel derived ferroelectric thin films, Journal of Applied Physics 95 (January 2004) 629–634.
[11] S. Corkovic, R. Whatmore, Q. Zhang, Development of residual stress in sol–gel derived $Pb(Zr,Ti)O_3$ films: an experimental study, Journal of Applied Physics 103 (April 2008) 084101.
[12] S. Sengupta, S. Park, D. Payne, L. Allen, Origins and evolution of stress development in sol–gel derived thin layers and multideposited coatings of lead titanate, Journal of Applied Physics 83 (February 1998) 2291–2296.
[13] E. Hong, R. Smith, S. Krishnaswamy, C. Freidhoff, S. Trolier-McKinstry, Residual stress development in $Pb(Zr,Ti)O_3/ZrO_2/SiO_2$ stacks for piezoelectric microactuators, Thin Solid Films 510 (January 2006) 213–221.
[14] T.A. Berfield, R.J. Ong, D.A. Payne, N.R. Sottos, Residual stress effects on piezoelectric response of sol–gel derived lead zirconate titanate thin films, Journal of Applied Physics 101 (2007), paper 024102.
[15] J.W. Lee, C.S. Park, M. Kim, H.E. Kim, Effects of residual stress on the electrical properties of PZT films, Journal of American Ceramic Society 90 (2007) 1077–1080.
[16] K. Yamashita, H. Nishimoto, M. Okuyama, Diaphragm deflection control of piezoelectric ultrasonic microsensors for sensitivity improvement, Sensors and Actuators A: Physical 139 (April 2007) 118–123.

[17] S. Lee, T. Tanaka, K. Inoue, Residual stress influences on the sensitivity of ultrasonic sensor having composite membrane structure, Sensors and Actuators A: Physical 125 (October 2006) 242–248.
[18] J. Pulskamp, A. Wickenden, R. Polcawich, B. Piekarski, M. Dubey, G. Smith, Mitigation of residual stress deformation in multilayer microelectromechanical systems cantilever devices, Journal of Vacuum Science & Technology B 21 (November 2003) 2482–2486.
[19] Y.C. Hsu, C.C. Wu, C.C. Lee, G.Z. Cao, I.Y. Shen, Demonstration and characterization of PZT thin-film sensors and actuators for meso- and micro-structures, Sensors and Actuators A: Physical 116 (3) (October 2004) 369–377.
[20] C. Lee, Q. Guo, G. Cao, I.Y. Shen, Effect of electrode size and silicon residue on piezoelectric thin-film membrane actuators, Sensors and Actuators A: Physical 147 (May 2008) 279–285.
[21] Q. Guo, G. Cao, I. Shen, Measurements of piezoelectric constant d_{33} of lead zirconate titanate oxide (PZT) through use of a mini impact hammer, in: Proceedings of the ASME 2009 Design Engineering Technical Conferences & Computers and Information in Engineering Conference, IDETC (DETC2009-86157), 2009.
[22] J. Choi, J. Jang, B. Hahn, D. Park, W. Yoon, J. Ryu, C. Park, Preparation of highly dense PZN–PZT thick films by the aerosol deposition method using Excess-PbO powder, Journal of the American Ceramic Society 90 (2007) 3389–3394.
[23] P. Gkotsis, P. Kirby, F. Saharil, J. Oberhammer, G. Stemme, Thin film crystal growth template removal: application to stress reduction in lead zirconate titanate microstructures, Applied Physics Letters 91 (2007) 163504.
[24] J. Lu, T. Kobayashi, Y. Zhang, R. Maeda, T. Mihara, Wafer scale lead zirconate titanate film preparation by sol–gel method using stress balance layer, Thin Solid Films 515 (2006) 1506–1510.
[25] C. Zinck, D. Pinceau, E. Defay, E. Delevoye, D. Barbier, Development and characterization of membranes actuated by a PZT thin film for MEMS applications, Sensors and Actuators A: Physical 115 (February 2004) 483–489.
[26] E. Hong, S. Trolier-McKinstry, R. Smith, S. Krishnaswamy, C. Freidhoff, Design of MEMS PZT circular diaphragm actuator to generate large deflections, Journal of Micromechanics and Microengineering 15 (4) (2006) 832–839.
[27] W. Soedel, Vibrations of Shells and Plates, 2nd ed., Marcel Dekker, Inc., 1993, ch. 6, pp. 146–148.
[28] K. Yao, S. Yu, F.E.H. Tay, Residual stress analysis in ferroelectric $Pb(Zr_{0.52}Ti_{0.48})O_3$ thin films fabricated by a sol–gel process, Applied Physics Letters 82 (2003) 4540–4542.